

## Supplementary Information

### Liquid Metal-based Process for Tuning Thermoelectric Properties of Bismuth Indium System

Moonika Sari Widjajana,<sup>a,b</sup> Shih-Hao Chiu,<sup>a,b</sup> Yuan Chi,<sup>b</sup> Mahroo Baharfar,<sup>b</sup> Jiewei Zheng,<sup>b</sup> Mohammad Bagher Ghasemian,<sup>a,b</sup> Saroj Kumar Bhattacharyya,<sup>c</sup> Jianbo Tang,<sup>\*b</sup> Md Arifur Rahim,<sup>\*a,b</sup> Kourosh Kalantar-Zadeh<sup>\*a,b</sup>

<sup>a</sup> *School of Chemical and Biomolecular Engineering, University of Sydney, Sydney, NSW, 2006, Australia*

<sup>b</sup> *School of Chemical Engineering, University of New South Wales (UNSW), Kensington, NSW, 2052, Australia*

<sup>c</sup> *Solid State Elemental Analysis Unit, Mark Wainwright Analytical Centre, University of New South Wales (UNSW) - Sydney, Kensington, NSW, 2052, Australia*

*\*Correspondence to: jianbo.tang@unsw.edu.au (J.T.), ma.rahim@unsw.edu.au (M.A.R), and kourosh.kalantarzadeh@sydney.edu.au (K.K.-Z.).*

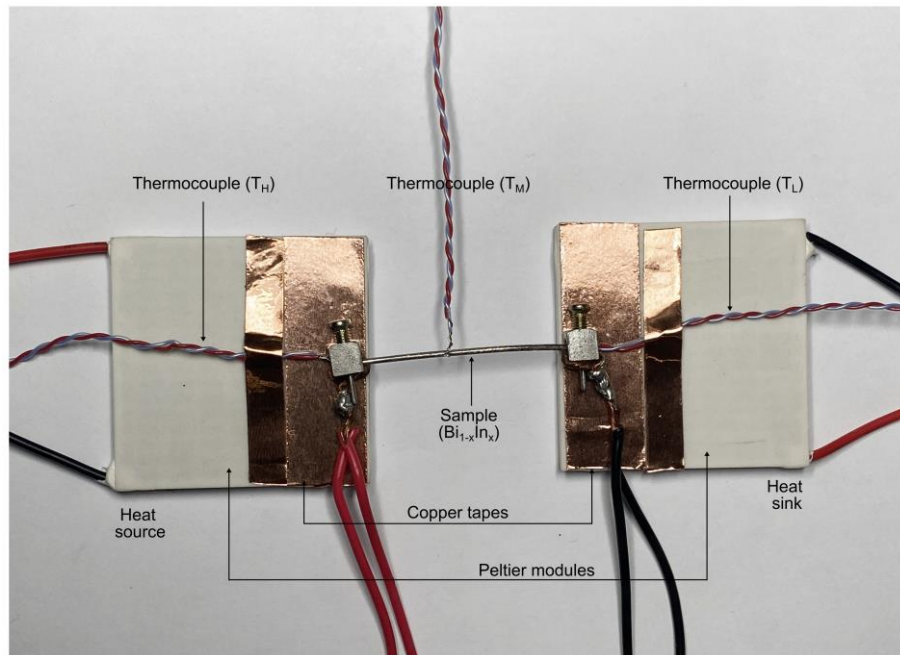


**Fig. S1** Experimental setup for measuring thermoelectric properties.

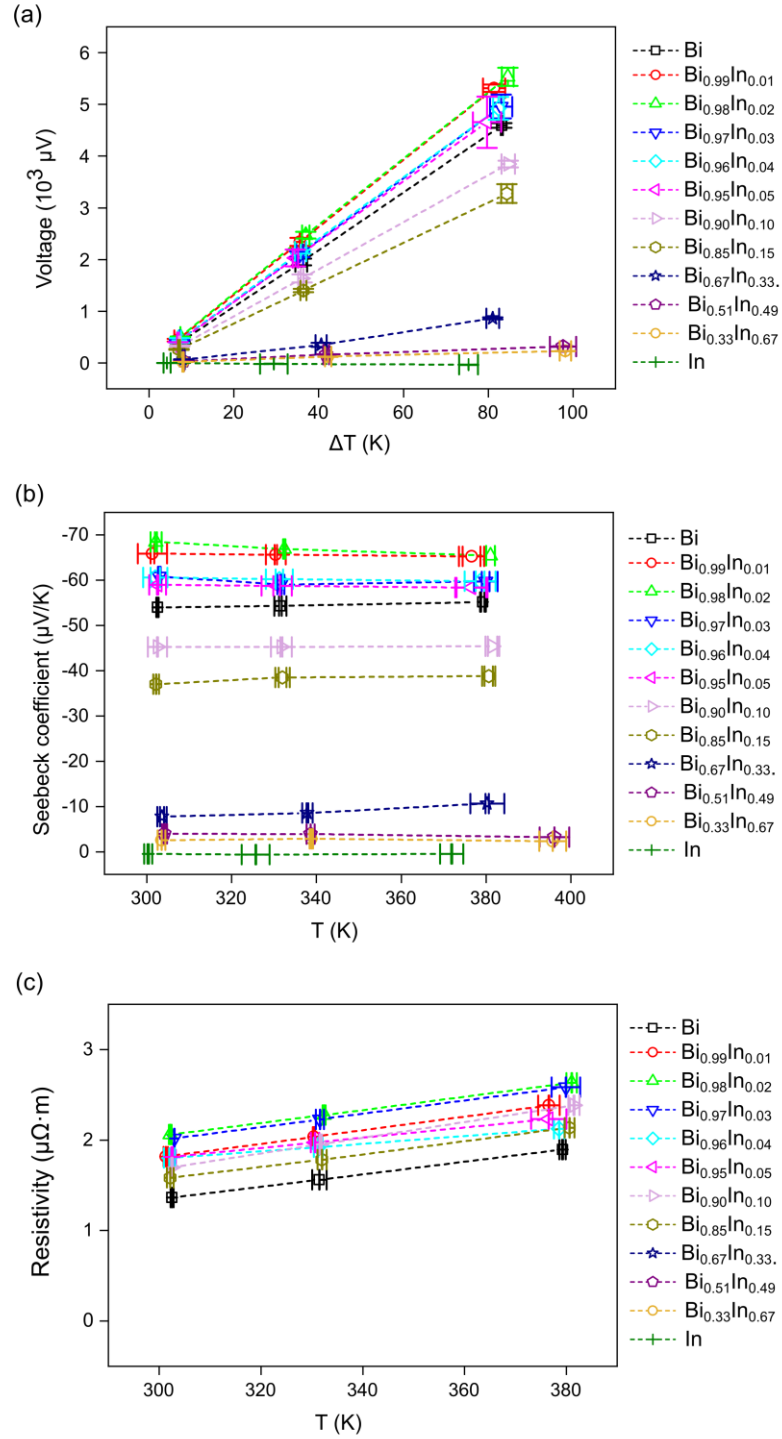


**Fig. S2** Thermoelectric properties of different Bi-In system: (a) The measured value of voltage vs  $\Delta$  temperature for Seebeck coefficient calculations, (b) temperature dependence of the Seebeck coefficient, and (c) temperature dependence of electrical resistivity values.

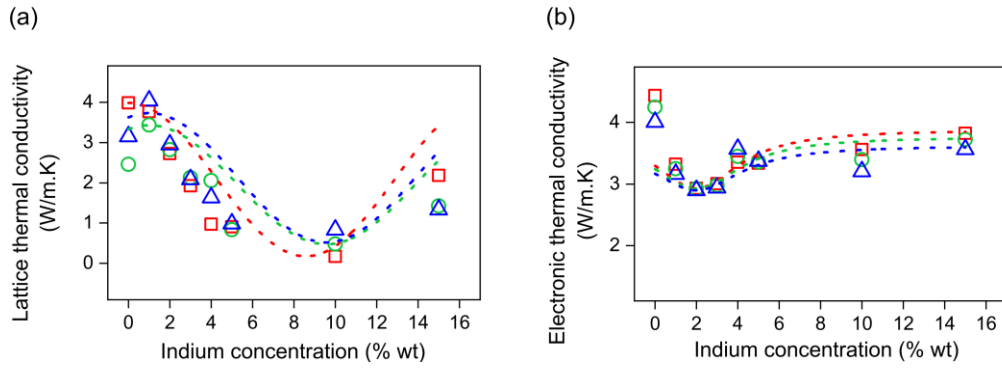


**Fig. S3** Thermoelectric properties of (a) Lattice thermal conductivity and (b) Electronic thermal conductivity in different indium concentration of samples. The symbols of red square, green circle, and blue triangle indicate that the hot end was kept at  $303\text{K} \pm 2\text{K}$ ,  $333\text{K} \pm 5\text{K}$ , and  $373\text{K} \pm 10\text{K}$ , respectively.

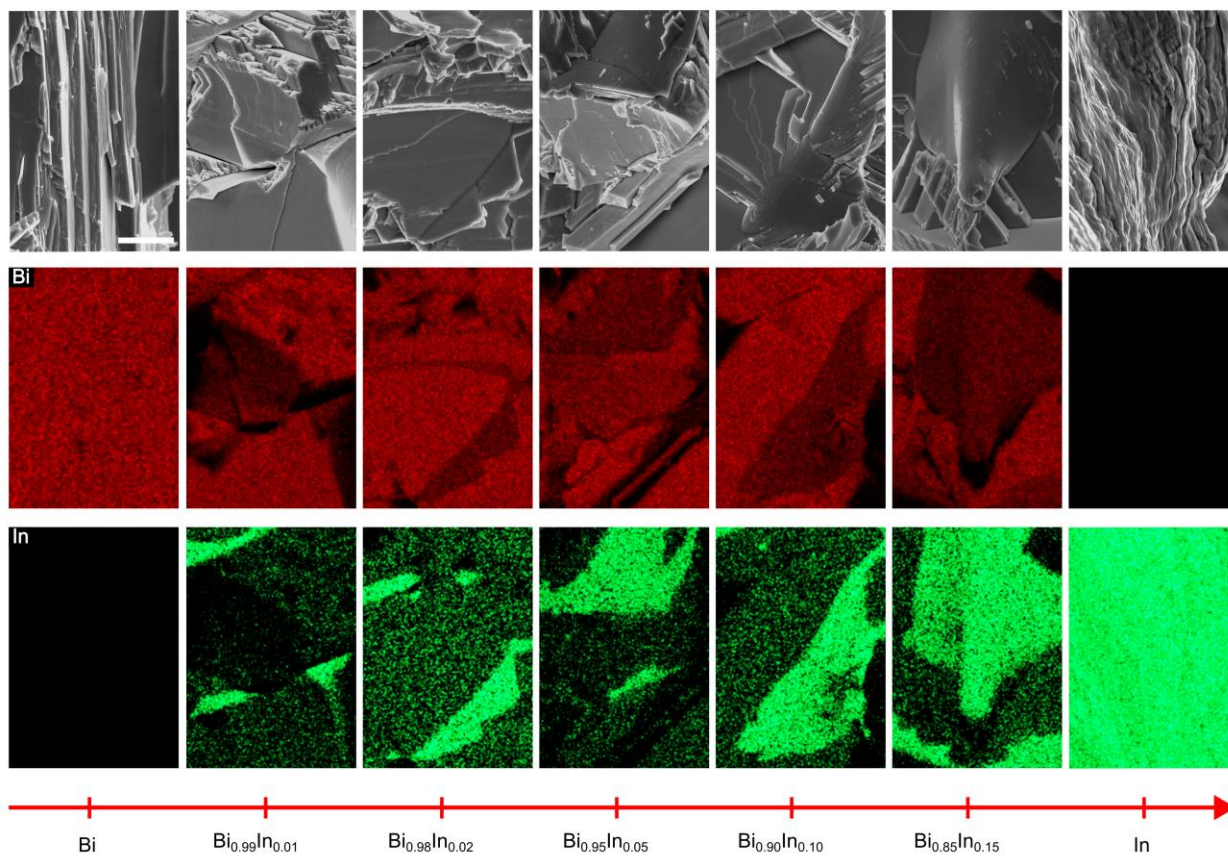


**Fig. S4** SEM/EDS images of the cross-sectional surfaces of different Bi-In samples. Scale bars in images are 10  $\mu\text{m}$ .

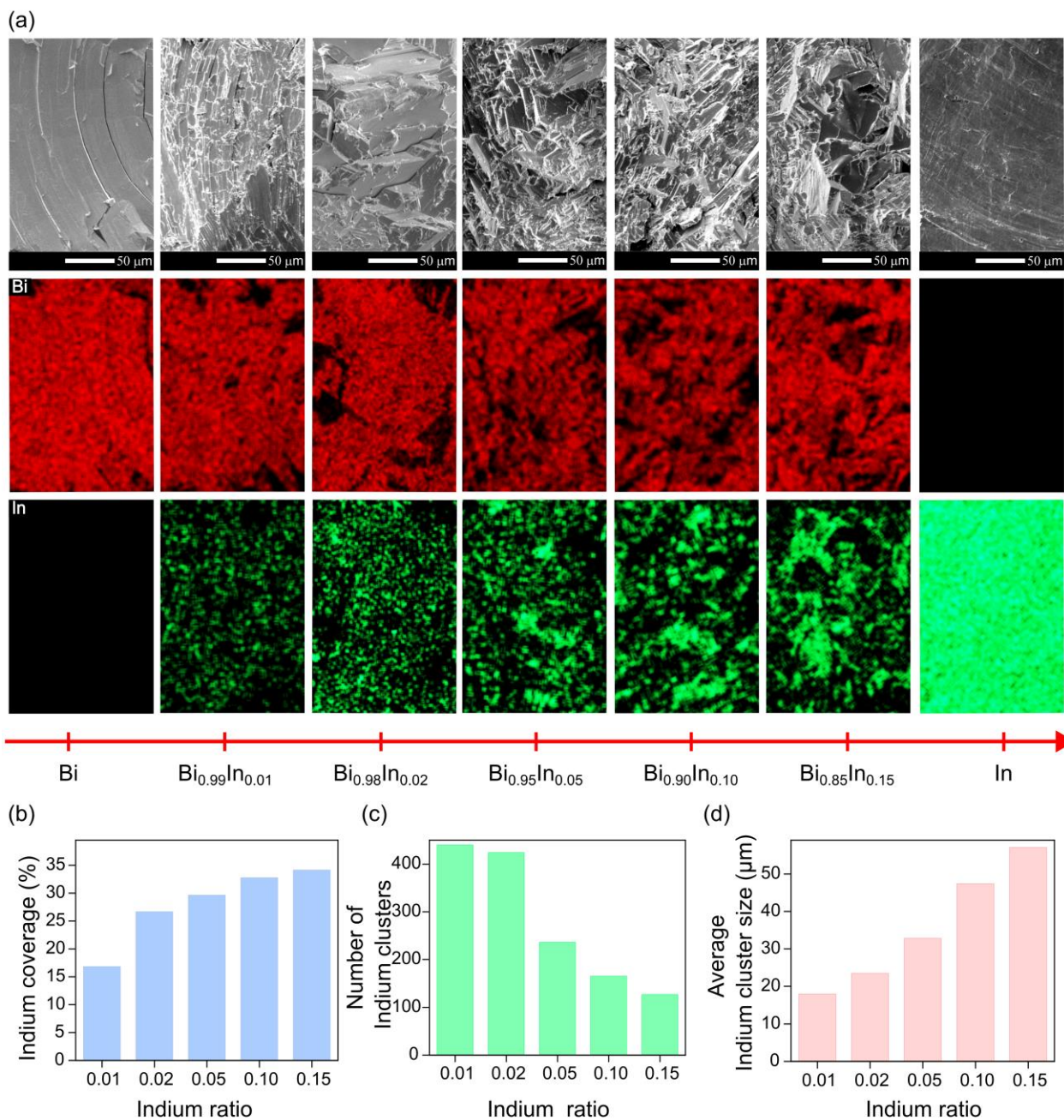


**Fig. S5** SEM/EDS analysis of the cross-sectional surfaces at a location different from the one in Fig. 4: (a) SEM images and elemental mappings of samples with different bismuth and indium concentrations. ImageJ Software Package analysis for (b) indium coverage (in mass ratio of the total sample), (c) number of indium clusters, and (d) average indium cluster size ( $\mu\text{m}$ ) across the cross sections.



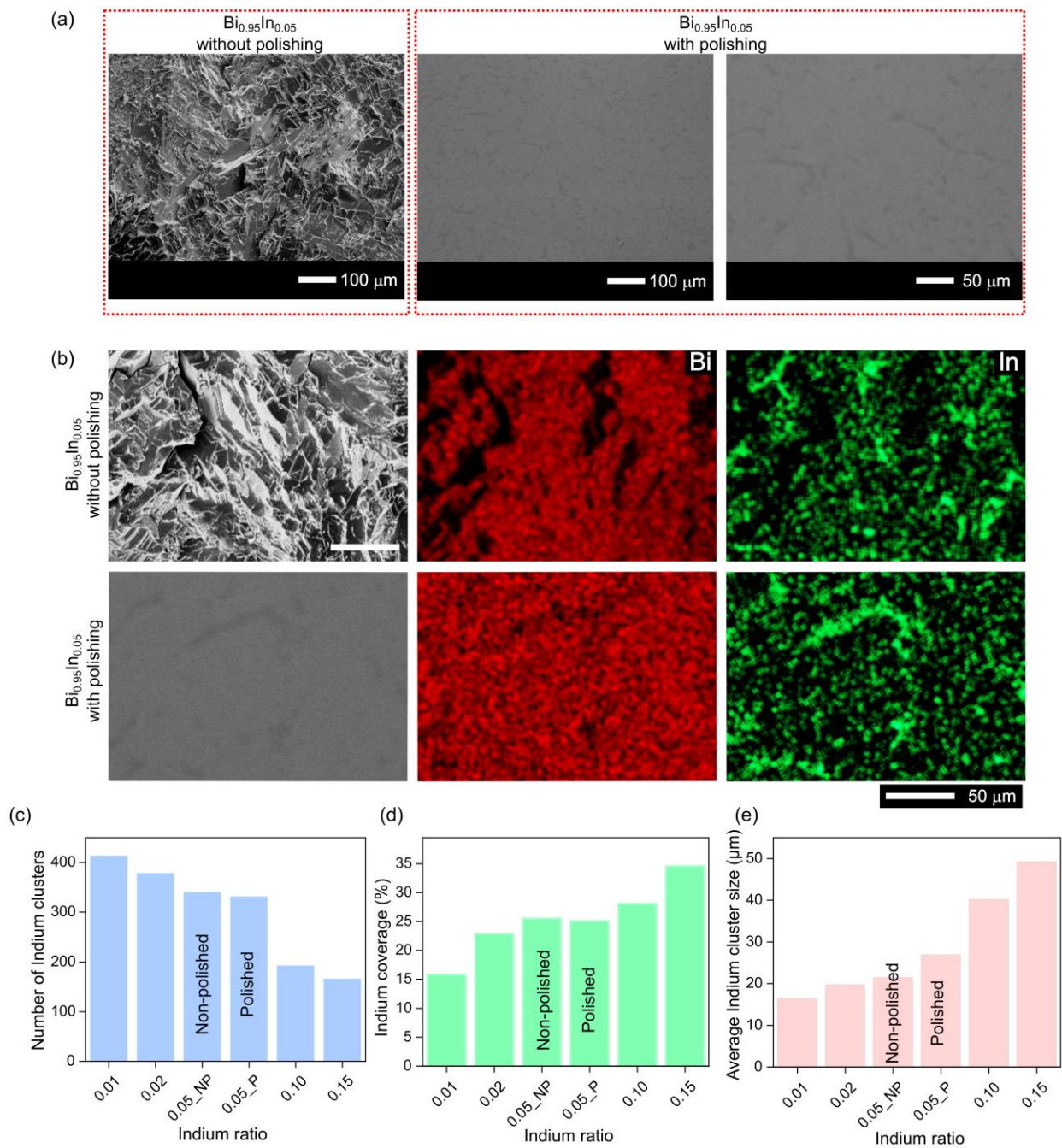


**Fig. S6** SEM/EDS analysis of the cross-sectional surfaces of  $\text{Bi}_{0.95}\text{In}_{0.05}$  samples for non-polished vs polished cross-sectional surface (a) SEM images in different magnifications (b) SEM images and elemental mappings of samples in 50  $\mu\text{m}$ , ImageJ Software Package analysis for (c) Indium coverage (in mass ratio of the total sample), (d) number of indium clusters, and (e) average indium cluster size ( $\mu\text{m}$ ) across the cross sections of various samples.

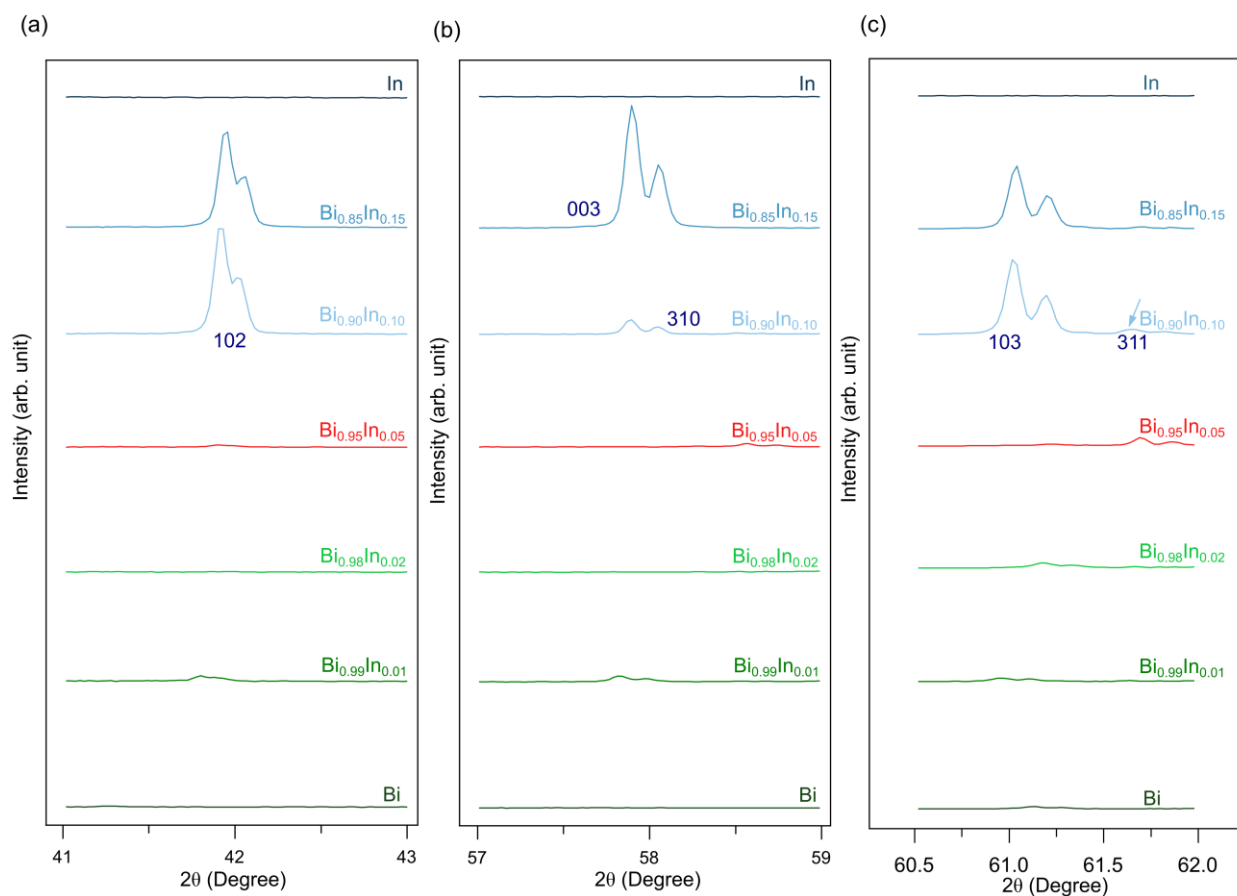


**Fig. S7** XRD patterns of different Bi-In samples in the zoomed ranges around: (a)  $41.8^\circ$  peak, (b)  $57.8^\circ$  peak and  $58.1^\circ$  peak, and (c)  $61.6^\circ$  peak.



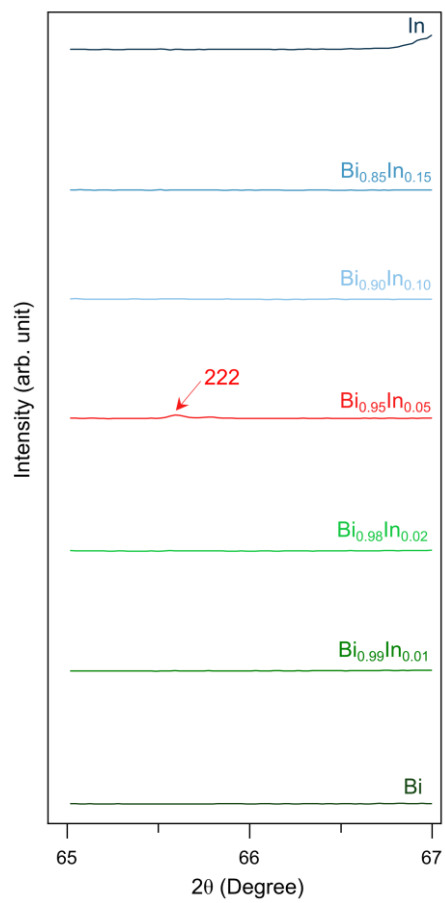


**Fig. S8** XRD patterns of different Bi-In samples in the zoomed ranges around 65.5° peak.

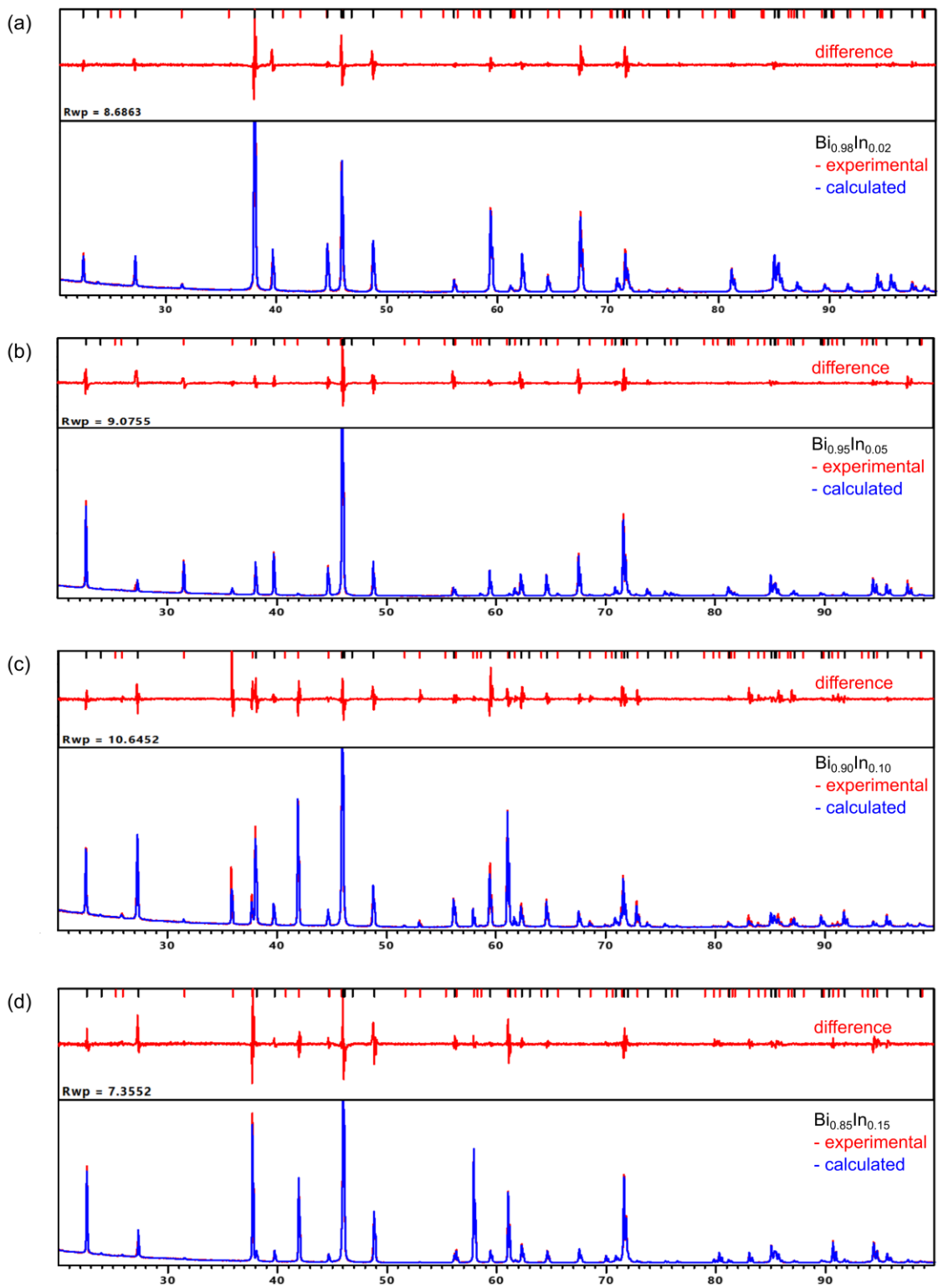


**Fig. S9** Full Rietveld XRD patterns of different Bi-In samples: (a)  $\text{Bi}_{0.98}\text{In}_{0.02}$  (b)  $\text{Bi}_{0.95}\text{In}_{0.05}$  (c)  $\text{Bi}_{0.90}\text{In}_{0.10}$ , and (d)  $\text{Bi}_{0.85}\text{In}_{0.15}$

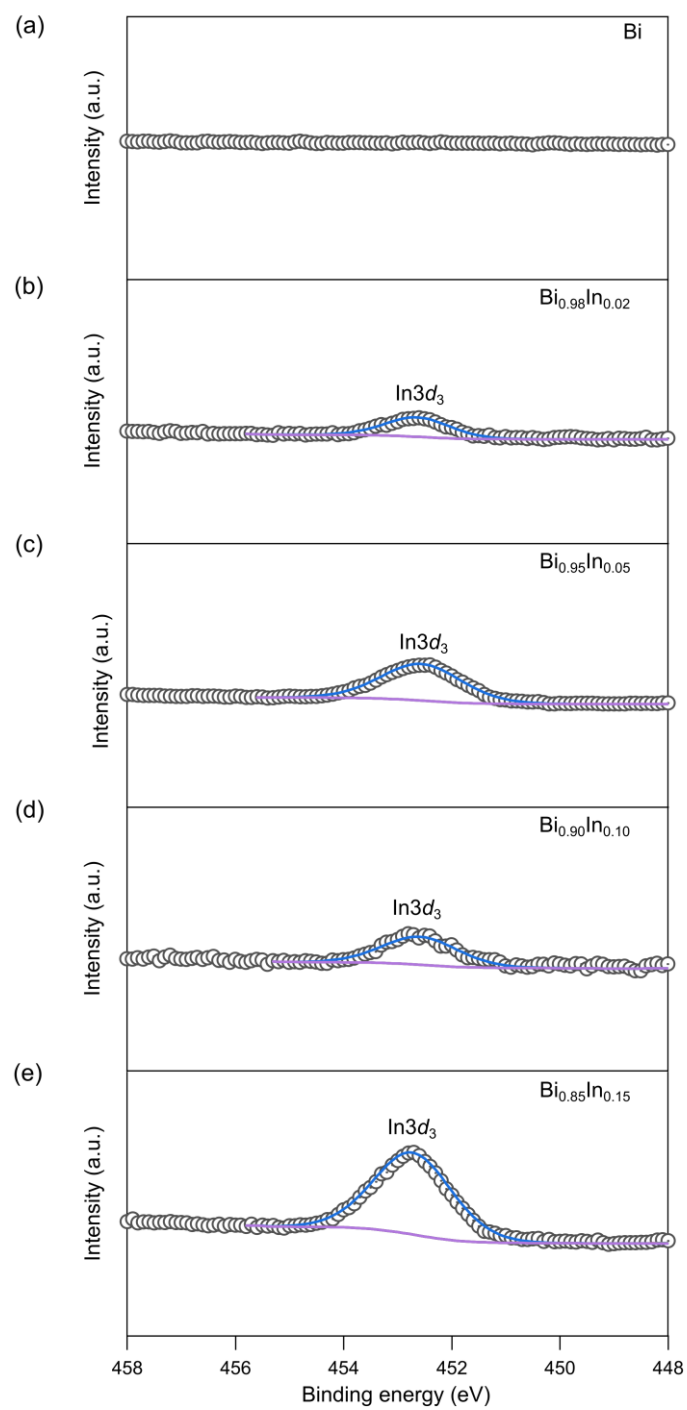


**Fig. S10** XPS patterns of In $3d_3$  spectra for: (a) Bi, (b) Bi<sub>0.98</sub>In<sub>0.02</sub>, (c) Bi<sub>0.95</sub>In<sub>0.05</sub>, (d) Bi<sub>0.90</sub>In<sub>0.10</sub>, and (e) Bi<sub>0.85</sub>In<sub>0.15</sub> systems.

**Table S1.** Reference values of thermoelectric properties for bismuth and indium elements.

Properties	Reference value	
	Bismuth	Indium
Melting point (°C) <sup>1,2</sup>	271.4	156.6
Seebeck coefficient (μV/K) <sup>3</sup>	-75.4	6.9
Electrical resistivity (nΩ·m) <sup>1,2</sup>	1068 (at 0 °C)	84 (at 0 °C)
Thermal conductivity (W/m·K) <sup>1,2</sup>	8.2 (at 0 °C)	71.1 (at 0 - 100 °C)

**Table S2.** Elemental quantitative analysis of cylindrical shaped of Bi-In systems using EDS and the calculation of Bi-In phase formed in the systems.

Sample	Mass Weight (%) Obtained by EDS		Bi and Bi-In phase (%) Calculated	
	Bi	In	Bi	Bi-In
Bi	100	0	100	0
Bi <sub>0.99</sub> In <sub>0.01</sub>	98.51	1.49	97.02	2.98
Bi <sub>0.98</sub> In <sub>0.02</sub>	97.89	2.11	95.78	4.22
Bi <sub>0.95</sub> In <sub>0.05</sub>	95.74	4.26	91.48	8.52
Bi <sub>0.90</sub> In <sub>0.10</sub>	89.65	10.35	79.3	20.7
Bi <sub>0.85</sub> In <sub>0.15</sub>	84.07	15.93	68.14	31.86
0	0	100	0	0



## References:

1. F. Habashi, in *Encyclopedia of Metalloproteins*, eds. R. H. Kretsinger, V. N. Uversky and E. A. Permyakov, Springer New York, New York, NY, 2013, DOI: 10.1007/978-1-4614-1533-6\_413, pp. 283-284.
2. F. Habashi, in *Encyclopedia of Metalloproteins*, eds. R. H. Kretsinger, V. N. Uversky and E. A. Permyakov, Springer New York, New York, NY, 2013, DOI: 10.1007/978-1-4614-1533-6\_416, pp. 981-982.
3. Q. Wang, M. Gao, L. Zhang, Z. Deng and L. Gui, *Sensors (Basel)*, 2019, **19**, 314.